Effects of Quantum Fluctuations on the Low-Energy Collective Modes of Two-Dimensional Superfluid Fermi Gases from the BCS to the Bose Limit

Senne Van Loon[1,2,*] and C. A. R. Sá de Melo[1]

[1]*School of Physics, Georgia Institute of Technology, Atlanta, Georgia 30332, USA*
[2]*TQC, Universiteit Antwerpen, Universiteitsplein 1, B-2610 Antwerpen, Belgium*

We investigate the effects of quantum fluctuations on the low-energy collective modes of two-dimensional (2D) *s*-wave Fermi superfluids from the BCS to the Bose limit. We compare our results to recent Bragg scattering experiments in 2D box potentials, with very good agreement. We show that quantum fluctuations in the phase and modulus of the pairing order parameter are absolutely necessary to give physically acceptable chemical potential and dispersion relation of the low-energy collective mode throughout the BCS to Bose evolution. Furthermore, we demonstrate that the dispersion of the collective modes change from concave to convex as interactions are tuned from the BCS to the Bose regime, and never crosses the two-particle continuum, because arbitrarily small attractive interactions produce bound states in two dimensions.

The study of collective modes is a fundamental component of many-particle physics, because for every spontaneously broken continuous symmetry there are low-energy modes that emerge as expected from Goldstone's theorem [1], and additional higher-energy excitations such as the Higgs mode [2,3]. Collective modes are essential in understanding a variety of systems ranging from condensed matter (quantum magnets, superconductors) [4,5], high energy physics (standard nuclear matter, quantum chromodynamics) [6,7], and astrophysics (neutron stars, black holes) [8,9] to atomic (Bose and Fermi superfluids) physics [10,11]. Unfortunately, in condensed matter it is not easy to tune parameters such as interactions, density, and dimensionality over a wide range, in high energy physics it is very difficult, and in astrophysics it is impossible. However, in atomic physics this is relatively easy via well established techniques [12,13]. This makes it possible to investigate collective modes in superfluids, particularly important because they reveal the effects of quantum fluctuations above the superfluid ground state.

Superfluids in 2D are inherently different from their 3D counterparts, due to the importance of fluctuations [14,15] leading to a Berezinskii-Kosterlitz-Thouless (BKT) transition [16,17]. In the context of ultracold atoms, the desire to study 2D Fermi superfluids is driven not only by connections to high-temperature superconductors [18–21], but also by the high degree of experimental control that allows the measurement of the equation of state [22–24], the observation of the BKT transition [25,26], and the examination of collective modes [27–30].

Ultracold fermions with tunable interactions in nearly 2D configurations were studied using harmonic traps and optical lattices [31–34]. With the very recent advent of box potentials, it is now possible to study experimentally homogeneous 2D fermions [28,30,35]. Inspired by recent measurements of collective excitations via Bragg-spectroscopy [30,36,37], we investigate the low-energy collective modes of 2D *s*-wave Fermi superfluids in box potentials, and find very good agreement with experiments. We establish that mean field (saddle point) results in two dimensions [38] produce incorrect values of the chemical potential and lead to the erroneous conclusion that the sound velocity is a constant throughout the BCS to Bose evolution [39–41]. In sharp contrast, we show that the inclusion of quantum fluctuations [42] is crucial to produce physically acceptable results for the dispersion of collective modes and leads to a varying speed of sound in the crossover from BCS to Bose regimes at low temperatures [43]. Furthermore, we demonstrate that phase and modulus fluctuations of the pairing order parameter become increasingly more coupled with growing interaction strength. Importantly, we clarify the longstanding confusion about the difference between the resulting sound mode arising from the broken U(1) symmetry and Landau's phenomenological first sound.

Based on weakly coupled *s*-wave Fermi superfluids and a linear dispersion of the collective mode, it has been long thought [44] that the low-energy collective modes in neutral Fermi superfluids are strongly damped (due to Landau damping) when the energy of the collective mode is sufficiently large to reach the pair-breaking energy threshold. In three dimensions, this view is still valid, even when taking into account the changing concavity of the dispersion [45,46]. However, we show that the situation is fundamentally different in two dimensions, where the inclusion of the ubiquitous bound states and of higher-order momentum corrections to the collective mode dispersion

show that the collective mode energy never reaches the two-particle continuum, and thus there is no damping of the collective mode at the Gaussian level for s-wave superfluids.

Hamiltonian.—To analyze the low-energy collective modes of 2D s-wave Fermi superfluids in box potentials, we start from the Hamiltonian density

$$\mathcal{H} = \psi_s^\dagger(\mathbf{r})\frac{(-i\hbar\nabla)^2}{2m}\psi_s(\mathbf{r}) - g\psi_\uparrow^\dagger(\mathbf{r})\psi_\downarrow^\dagger(\mathbf{r})\psi_\downarrow(\mathbf{r})\psi_\uparrow(\mathbf{r}), \quad (1)$$

where $\psi_s(\mathbf{r})$ is a fermion field operator with spin s at position $\mathbf{r}$. The first term is the kinetic energy and the second represents local attractive interactions. The associated action is $\mathcal{S}(\psi^\dagger, \psi) = \int d^3r\{\psi^\dagger(r)[\hbar\partial_\tau - \mu]\psi(r) + \mathcal{H}(r)\}$, where $r = (\mathbf{r}, \tau)$, $\int d^3r = \int_0^\beta d\tau \int d^2\mathbf{r}$, $\beta = \hbar/k_BT$, and μ is the chemical potential. The grand canonical partition function of the system is $\mathcal{Z} = \int D\psi^\dagger D\psi e^{-\mathcal{S}/\hbar}$. We introduce the Hubbard-Stratonovich complex pair field $\Phi(r)$ to decouple the contact interactions and integrate out the fermionic fields to obtain an effective action $S_{\text{eff}}(\Phi^\dagger, \Phi)$. We write $\Phi(r) = |\Phi(r)|e^{i\theta(r)}$ in terms of its modulus $|\Phi(r)| = |\Delta|[1 + \lambda(r)]$ and phase $\theta(r)$, and expand $S_{\text{eff}}(\Phi^\dagger, \Phi)$ up to quadratic order in both the phase $\theta(r)$ and modulus fluctuations $\lambda(r)$ around the saddle point $|\Phi_{\text{sp}}(r)| = |\Delta|$. The resulting Gaussian action is

$$S_{\text{eff}} = S_{\text{sp}} + \beta|\Delta|^2 \sum_q \begin{pmatrix} i\theta_{-q} & \lambda_{-q} \end{pmatrix} M(q) \begin{pmatrix} -i\theta_q \\ \lambda_q \end{pmatrix}, \quad (2)$$

where $q = (\mathbf{q}, i\nu)$ and $\nu = 2\pi n/\beta$ are bosonic Matsubara frequencies, $S_{\text{sp}} = \beta\sum_{\mathbf{k}}(\xi_{\mathbf{k}} - E_{\mathbf{k}}) + \beta L^2|\Delta|^2/g$ is the saddle-point action, and $M(q)$ is the symmetric Gaussian fluctuation matrix [47]. Using the analytic continuation $i\nu \to \omega + i\delta$, the matrix elements of $M(q)$, at zero temperature, are

$$\frac{M_{\pm\pm}}{L^2} = \int \frac{d^2\mathbf{k}}{4\pi^2}\left[\frac{E_+ + E_-}{2E_+E_-}\frac{E_+E_- + \xi_+\xi_- \pm |\Delta|^2}{\hbar^2\omega^2 - (E_+ + E_-)^2} + \frac{1}{2E_{\mathbf{k}}}\right],$$

$$\frac{M_{+-}}{L^2} = \int \frac{d^2\mathbf{k}}{4\pi^2}\left[\frac{\hbar\omega}{2E_+E_-}\frac{E_+\xi_- + \xi_+E_-}{\hbar^2\omega^2 - (E_+ + E_-)^2}\right],$$

where $E_{\mathbf{k}} = \sqrt{\xi_{\mathbf{k}}^2 + |\Delta|^2}$ is the quasiparticle energy, $\xi_{\mathbf{k}} = \epsilon_{\mathbf{k}} - \mu$ is the energy of the free fermions of mass m ($\epsilon_{\mathbf{k}} = \hbar^2|\mathbf{k}|^2/2m$) with respect to μ, and $|\Delta|$ is the modulus of the order parameter. We have used the shorthand notations $E_\pm = E_{\mathbf{k}\pm\mathbf{q}/2}$ and $\xi_\pm = \xi_{\mathbf{k}\pm\mathbf{q}/2}$, $M_{++} = M_{\theta\theta}$, $M_{--} = M_{\lambda\lambda}$, and $M_{+-} = M_{\theta\lambda}$.

Equation of state.—In Eq. (2), the action S_{eff} is fully characterized by $|\Delta|$ and μ or by the dimensionless parameters $x = \mu/|\Delta|$ and $|\Delta|/\epsilon_F$, where ϵ_F is the Fermi energy for a specified density $n = k_F^2/2\pi$, with k_F being the Fermi momentum. However, to study the evolution from the BCS to the Bose limit, it is experimentally more relevant to relate
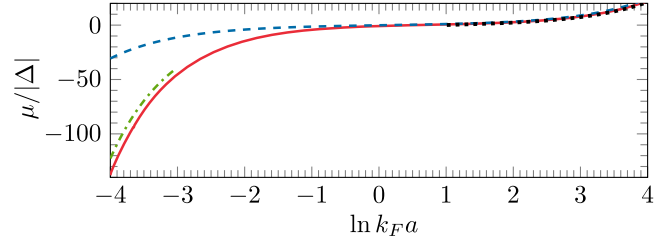
FIG. 1. The ratio $x = \mu/|\Delta|$ for different approximations of the equation of state: the saddle-point approximation (dashed blue line) and including Gaussian fluctuations (solid red line). The BCS and Bose limits are shown as dotted black and dot-dashed green lines.

$|\Delta|$ and μ to the 2D scattering length a and the density n. The order parameter is found from $[\partial\Omega_{\text{sp}}/\partial|\Delta|]_{T,V} = 0$, where $\Omega_{\text{sp}} = S_{\text{sp}}/\beta$ is the saddle-point thermodynamic potential. Replacing the interaction strength g in favor of the (positive) two-body binding energy ϵ_b, using the Lippmann-Schwinger relation $L^2/g = \sum_{\mathbf{k}} 1/(2\epsilon_{\mathbf{k}} + \epsilon_b)$ [48], one finds $|\Delta| = \sqrt{\epsilon_b(2\mu + \epsilon_b)}\Theta(2\mu + \epsilon_b)$, which is explicitly only a function of μ and ϵ_b. The chemical potential can be found by solving the saddle-point number equation $n_{\text{sp}} = -[\partial\Omega_{\text{sp}}/\partial\mu]_{T,V}/L^2$, while fixing the density $n_{\text{sp}} = n = k_F^2/2\pi$, resulting in $\mu_{\text{sp}} = \epsilon_F - \epsilon_b/2$, which substituted in the order parameter relation leads to $|\Delta|_{\text{sp}} = \sqrt{2\epsilon_F\epsilon_b}$. These expressions are connected to the 2D scattering length a via the relation $\epsilon_b = 8\epsilon_F/\exp(2\gamma_E + 2\ln k_Fa)$, with $\gamma_E \approx 0.577$ the Euler-Mascheroni constant [49]. However, as discussed below, this analysis leads to the unphysical result of a constant sound velocity $c = v_F/\sqrt{2}$, where v_F is the Fermi velocity, over the entire BCS-to-Bose evolution, because μ is inaccurately calculated.

A more precise determination of μ for fixed density n requires not only Ω_{sp}, but also the Gaussian contribution $\Omega_g = (k_BT/2)\sum_q \ln\det[|\Delta|M(q)]$, found by integrating the bosonic fields in the second term of Eq. (2). The full number equation $n = n_{\text{sp}} + n_g$, including fluctuations of the order parameter at the Gaussian level, is necessary to determine μ. This is important both in three [50,51] and two dimensions [42,48]. Here, $n_g = -[\partial\Omega_g/\partial\mu]_{T,V}/L^2$ must be always positive and $n(\mu) = k_F^2/2\pi$ must be solved numerically, leading to a significant reduction of μ in the Bose regime [52], see Fig. 1.

Collective modes.—As seen from Eq. (2), the fluctuation matrix $M(q)$ acts as the inverse propagator of modulus and phase fluctuations. The collective mode frequency $\omega_{\mathbf{q}}$ is found from the poles of $[M(q)]^{-1}$ or, equivalently, from $\det M(\mathbf{q}, \omega_{\mathbf{q}}) = 0$ [47]. As shown in the Supplemental Material [53], at $T = 0$, these poles are identical to the poles of the density-density response function, as probed by experiments measuring the dynamical structure factor [30].
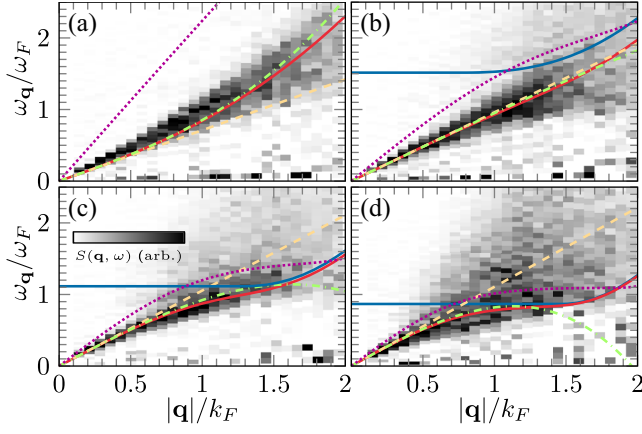
FIG. 2. Frequency $\omega_{\mathbf{q}}$ vs $|\mathbf{q}|$, using Fermi units $\omega_F = \epsilon_F/\hbar$ and k_F, for different interactions. The solid red line represents the numerical solution for $\omega_{\mathbf{q}}$, while the analytical approximation is shown up to linear (dashed yellow line) and cubic (dot-dashed green line) order in $|\mathbf{q}|$. The parameters for each panel are (a) $\ln k_F a = -0.1, (\mu/|\Delta| \simeq -1.0)$, (b) $\ln k_F a = 0.7, (\mu/|\Delta| \simeq 0.2)$, (c) $\ln k_F a = 1.1, (\mu/|\Delta| \simeq 0.7)$, and (d) $\ln k_F a = 1.4, (\mu/|\Delta| \simeq 1.2)$, using the Gaussian value of μ. The dotted magenta lines represent $\omega_{\mathbf{q}}^{\mathrm{PO}}$ using the saddle point μ. The solid blue line indicates the lower edge of the two-particle continuum $\epsilon_c(\mathbf{q})$ at the Gaussian level. Our results are compared to dynamic structure factor experiments (gray pixels) from Ref. [30], showing very good agreement.

A real solution is found below the two-particle continuum $\epsilon_c(\mathbf{q}) = \min_{\mathbf{k}}(E_+ + E_-)$, above which it is energetically more favorable to break pairs. In a 3D Fermi gas, $\omega_{\mathbf{q}}$ can hit the two-particle continuum at some finite value of $\mathbf{q}$ causing damping [45]. However, for a 2D Fermi gas, a real $\omega_{\mathbf{q}} < \epsilon_c(\mathbf{q})$ is found for all values of $\mathbf{q}$, given that a two-body bound state always exists for a 2D contact potential [66]. This physics arises from $M_{++} = M_{\theta\theta}$, which always diverges when $\hbar\omega \to \epsilon_c$ making $\det M(\mathbf{q}, \epsilon_c) = 0$ impossible, and thus there is no damping of the mode at the Gaussian level. (See Supplemental Material [53] for an in-depth discussion on damping.) For arbitrary $\mathbf{q}$ there is no general analytical solution for $\omega_{\mathbf{q}}$, but we obtain numerical results shown as solid red lines in Fig. 2. We compare our results to the measured spectrum from Ref. [30], and find that $\omega_{\mathbf{q}}$ follows closely the maximum of the dynamical structure factor, without any fitting parameters. Moreover, it can be seen that $\omega_{\mathbf{q}}$ avoids the two-particle continuum $\epsilon_c(\mathbf{q})$ and that a solution exists for all $\mathbf{q}$.

Although numerical solutions are useful for comparison to recent experiments [28,30], analytical insight is essential to understand the underlying physics. To reveal the interplay between modulus and phase fluctuations, we show next that their coupling increases dramatically as the system evolves from the BCS to the Bose regime. We invert $M(q)$ and obtain the propagators in Fourier space, which in the long wavelength limit become
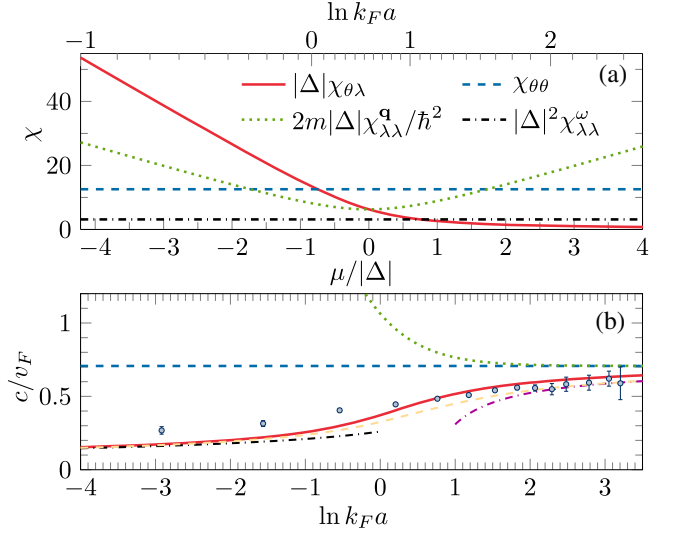
FIG. 3. (a) Different χ coefficients vs $\mu/|\Delta|$ or $\ln k_F a$ as defined in Eq. (3). (b) Sound velocity c/v_F vs $\ln k_F a$: the dotted green line includes phase-only fluctuations with saddle point μ, diverging in the Bose limit; blue dashed line includes phase and modulus fluctuations with saddle point μ, giving always a constant value; solid red line combines phase and modulus fluctuations with Gaussian μ self-consistently. The dot-dashed magenta and black lines show the results in the BCS and Bose limits, respectively. We compare our broken-U(1) sound velocity c with the experimental results of the isentropic sound velocity u_S from Ref. [28] (blue circles), and with c from Eq. (4) and the Monte Carlo equation of state from Ref. [67] (dashed yellow line). See an in-depth discussion of the conceptual difference between c and u_S in the Supplemental Material [53].

$$\begin{pmatrix} \langle\theta_{-q}\theta_q\rangle & \langle\theta_{-q}\lambda_q\rangle \\ \langle\lambda_{-q}\theta_q\rangle & \langle\lambda_{-q}\lambda_q\rangle \end{pmatrix}$$
$$= \frac{|\Delta|^2}{\hbar^2 c^2 q^2 - \hbar^2\omega^2} \begin{pmatrix} \chi_{\theta\theta} & i\hbar\omega\chi_{\theta\lambda} \\ -i\hbar\omega\chi_{\theta\lambda} & q^2\chi_{\lambda\lambda}^{\mathbf{q}} - \hbar^2\omega^2\chi_{\lambda\lambda}^{\omega} \end{pmatrix}. \quad (3)$$

The different χ coefficients defined in this equation are shown in Fig. 3(a) as a function of interaction parametrized by the ratio $x = \mu/|\Delta|$. They are explicitly given by $\chi_{\theta\theta} = 4\pi$, $\chi_{\theta\lambda} = 2\pi(-x + \sqrt{1 + x^2})/|\Delta|$, $\chi_{\lambda\lambda}^{\mathbf{q}} = \hbar^2\pi\sqrt{1 + x^2}/2m|\Delta|$, and $\chi_{\lambda\lambda}^{\omega} = \pi/|\Delta|^2$. Most notably, the solid red line in Fig. 3(a) shows $\chi_{\theta\lambda}$, which controls the coupling between phase and modulus. Notice that $\chi_{\theta\lambda}$ is large in the Bose regime $(\mu/|\Delta| \ll -1)$, indicating that phase and modulus are strongly mixed, while it is negligible in the BCS regime $(\mu/|\Delta| \gg 1)$, showing that phase and modulus are essentially decoupled. For $\omega > 0$, the pole of $[M(|\mathbf{q}|, \omega)]^{-1}$ occurs at $\omega_{\mathbf{q}} = c|\mathbf{q}|$, with

$$2mc^2 = \mu + \sqrt{\mu^2 + |\Delta|^2}, \quad (4)$$

where c is the sound velocity associated with the broken U(1) symmetry. This expression includes modulus and phase

fluctuations of the order parameter, and explicitly illustrates the dependence of c on μ. In Fig. 3(b), we show the behavior of c/v_F at three levels of approximation: the dotted green line includes only phase fluctuations, the dashed blue line includes phase and modulus fluctuations with the saddle-point value of μ, while the solid red line includes phase and modulus fluctuations with a self-consistent Gaussian fluctuation value of μ. It is clear that the first two levels of approximation [39,40] give completely unphysical results, in particular predicting the constant value $c = v_F/\sqrt{2}$ for any coupling in the saddle-point approximation, as quoted in the literature [39,40]. However, we show here that the inclusion of phase and modulus fluctuations with the correct μ leads to the appropriate behavior of c both in the Bose and BCS limits, giving results that are surprisingly close to the experimentally measured isentropic sound velocity [28], that is typically a good estimate for Landau's first sound.

The sound mode arising from the broken U(1) symmetry should not be confused with Landau's first or second sound [68], as they are fundamentally different. Our $T = 0$ microscopic collective mode can be directly observed in measurements of the dynamic structure factor, and exists in the collisionless regime. Conversely, first and second sound result from a phenomenological decomposition of the superfluid into two components, and exist only in the hydrodynamic regime [69,70]. In clarifying the difference between the broken-U(1) and Landau's first sound, we show that Landau's first sound velocity is always larger than c, see Supplemental Material [53]. We also note that the isentropic sound velocity [28] is not the same as the sound velocity that can be extracted from the dynamical structure factor [30].

Further insight is gained by studying the long wavelength limit of S_{eff} in Eq. (2) by expanding the fluctuation matrix $M(\mathbf{q}, \omega)$ for small $\mathbf{q}$ and ω. Performing an inverse Fourier transform back to real space, the second term in Eq. (2) reduces to

$$S_g = \frac{1}{2}\int d^3 r[\rho_s(\nabla\theta)^2 + A(\hbar\partial_\tau\theta)^2 + iD\lambda\hbar\partial_\tau\theta + C\lambda^2]. \quad (5)$$

The first two coefficients are the $T = 0$ superfluid density $2m\rho_s/\hbar^2 = n_{\text{sp}}/2$ and the compressibility $A = (1 + x/\sqrt{1 + x^2})m/8\pi\hbar^2$, while $D = m|\Delta|/\sqrt{1 + x^2}/2\pi\hbar^2$ controls the phase-modulus coupling, and $C = |\Delta|^2(1 + x/\sqrt{1 + x^2})m/2\pi\hbar^2$ describes the mass term for the modulus fluctuations. Neglecting modulus fluctuations ($\lambda = 0$) leads to a sound velocity $c = \sqrt{\rho_s/A}/\hbar = (\mu^2 + |\Delta|^2)^{1/4}/\sqrt{m}$, shown as the dotted green line in Fig. 3(b), which diverges in the Bose limit. However, when $\lambda \neq 0$, the coupling between modulus and phase renormalizes A. Integrating out λ leads to a renormalized phase-only action with unchanged superfluid density $\rho_{sR} = \rho_s$, but renormalized

compressibility $A_R = A + D^2/4C = m/4\pi\hbar^2$. This renormalization leads to the corrected speed $c = \sqrt{\rho_{sR}/A_R}/\hbar$ given by Eq. (4), as expected. This moreover leads to the conclusion that the collective mode studied here is neither a Goldstone (pure phase) nor Higgs (pure modulus) mode, because the mixing of phase and modulus cannot be neglected.

Change in concavity.—To investigate the low-energy collective modes beyond linear dispersion, it is necessary to expand $M_{\pm\pm}$ and M_{+-} up to sixth order in ω and $|\mathbf{q}|$. In this case, the condition $\det M(\mathbf{q}, \omega_{\mathbf{q}}) = 0$ leads to

$$\omega_{\mathbf{q}} = c|\mathbf{q}|\left[1 + \frac{\gamma}{8}\left(\frac{\hbar|\mathbf{q}|}{mc}\right)^2 + \frac{\eta}{16}\left(\frac{\hbar|\mathbf{q}|}{mc}\right)^4 + \mathcal{O}\left(\frac{\hbar|\mathbf{q}|}{mc}\right)^6\right], \quad (6)$$

where the coefficients of the cubic and quintic order corrections have analytic expressions

$$\gamma = \frac{1}{24}\left(1 - 4x^2 - x\frac{7 + 4x^2}{\sqrt{1 + x^2}}\right), \quad (7)$$

$$\eta = -\frac{365 + 2802x^2 + 2048x^4 + 160x^6}{23040(1 + x^2)}$$
$$- x\frac{685 + 1813x^2 + 1064x^4 + 80x^6}{11520(1 + x^2)^{3/2}}. \quad (8)$$

In Fig. 2, we show $\omega_{\mathbf{q}}$ for various interaction regimes and different levels of approximation. The solid red curves represent the full numerical solutions, while the other curves represent the linear (dashed yellow) and cubic (dot-dashed green) approximations in $|\mathbf{q}|$ with the Gaussian corrected μ. The dotted line represents the numerical phase-only ($\lambda = 0$) dispersion $\omega_{\mathbf{q}}^{PO}$ using the saddle-point value of μ. Notice that $\omega_{\mathbf{q}}^{PO}$ severely overestimates the correct $\omega_{\mathbf{q}}$ in the Bose regime, that is, $\omega_{\mathbf{q}}^{PO} \gg \omega_{\mathbf{q}}$, while in the BCS limit $\omega_{\mathbf{q}}^{PO} \approx \omega_{\mathbf{q}}$, because the modulus and phase fluctuations are nearly decoupled. The panels in Fig. 2 show that there is a change in curvature in the solid red lines, also found in 3D Fermi gases [37,45–47], where the dispersion $\omega_{\mathbf{q}}$ is supersonic ($\gamma > 0$) in the Bose regime shown in panel (a), and subsonic ($\gamma < 0$) in the BCS regime shown in panel (d), where it bends downwards due to the pair-breaking continuum. The coefficients of the nonlinear terms play a significant role at larger momenta. While the cubic correction gives a good approximation for the large momentum behavior in the Bose limit, as one moves towards the BCS regime, progressively higher-order terms are needed to produce the appropriate behavior.

The coefficients γ and η are presented in Fig. 4 as a function of $\ln k_F a$. In all panels, γ and η are evaluated at different levels of approximation: the dotted green lines describe phase-only fluctuations using the saddle point μ, the dashed blue lines include modulus and phase
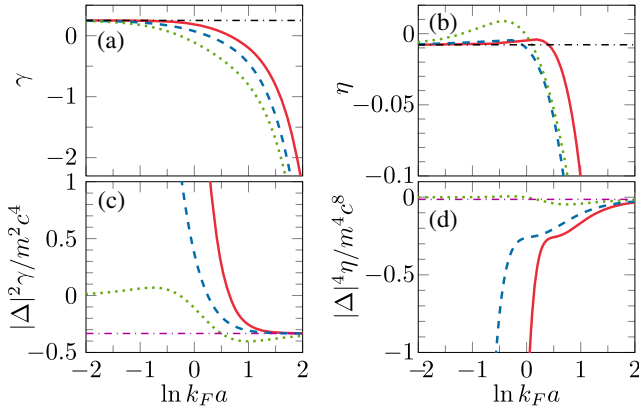
FIG. 4. Parameters γ and η vs $\ln k_F a$ at different levels of approximation: Phase-only fluctuations with saddle point μ (dotted green lines), phase and modulus fluctuations with saddle point μ (dashed blue lines), and with Gaussian corrected μ (solid red lines). The dot-dashed black and magenta lines describe the Bose and BCS limits. In (c) and (d), γ and η are scaled to reveal their behavior in the BCS limit.

fluctuations using the saddle point μ, and the solid red lines include modulus and phase fluctuations using the Gaussian μ. Panels (a)–(b) [(c)–(d)] show γ and η in units that elucidate their limiting behavior in the Bose (BCS) regime given by the dot-dashed black (magenta) lines.

The concavity of $\omega_{\mathbf{q}}$ is controlled by γ, which changes from $\gamma > 0$ (convex) to $\gamma < 0$ (concave) in the Bose and BCS regimes, respectively. The parameter γ changes sign at $x = \sqrt{(2\sqrt{13} - 7)/12} \approx 0.133$, corresponding to $\ln k_F a \simeq 0.65$ using the Gaussian μ. In this case ($\gamma = 0$), the first correction to the linear spectrum is a quintic ($|\mathbf{q}|^5$) term controlled by η. Although the behavior of γ and η is similar to the 3D results in the Bose limit [46], in the rest of the crossover the 2D case is qualitatively different, where η always stays negative because of the strong level repulsion with the two-particle continuum, due to the existence of two-body bound states for all interactions.

In the Bose limit ($x \ll -1$), expanding the matrix elements of $M(\mathbf{q}, \omega)$ to order $(\Delta/|\mu|)^2$ and to lowest order in $\hbar|\mathbf{q}|/\sqrt{2m|\mu|}$ leads to

$$\hbar^2(\omega_{\mathbf{q}}^{\mathrm{B}})^2 = \frac{\hbar^2 q^2}{2m_B}\left(\frac{\hbar^2 q^2}{2m_B} + 2m_B c_B^2\right), \qquad (9)$$

where $c_B = |\Delta|/\sqrt{2m_B|\mu|}$ is the Bogoliubov speed of sound, and $m_B = 2m$ is the boson mass. Using the saddle point μ leads to the incorrect value $c_B = v_F/\sqrt{2}$, while using the Gaussian corrected μ leads to $c_B = v_F/\sqrt{8|\ln k_F a|}$ in the Bose limit. The Bogoliubov-Popov interaction energy $2n_B V_B(0) = 2m_B c^2 = E_F/|\ln k_F a|$, with boson density $n_B = n/2$ leads to the boson-boson interaction parameter

$V_B(0) = (E_F/n)/|\ln k_F a|$. The values of γ and η from Eq. (9) are equal to limiting results obtained from Eqs. (7) and (8), that is, $\gamma \to 1/4$, and $\eta \to -1/128$, as seen in Figs. 4(a) and 4(b).

In the BCS limit ($x \gg 1$), the saddle point and Gaussian correction tend to the same results, as fluctuations are less important. Rescaling energies by $|\Delta|$, such that $\hbar\omega_{\mathbf{q}}/|\Delta|$ tends to a universal function of $\hbar c|\mathbf{q}|/|\Delta|$, leads to $(|\Delta|/mc^2)^2\gamma \to -1/3$ and $(|\Delta|/mc^2)^4\eta \to -1/72$, as revealed in Figs. 4(c) and 4(d). This is a consequence of the two-particle continuum pushing down the collective mode branch [45,46]. In this case, the expansion in $|\mathbf{q}|$ is limited to $\hbar c|\mathbf{q}| \leq 2|\Delta|$ and $c \to v_F/\sqrt{2}$.

Conclusions.—We analyzed low-energy collective modes of 2D s-wave Fermi superfluids from the BCS to the Bose regime giving excellent results when compared to Bragg spectroscopy experiments in 2D box potentials. We showed that quantum fluctuations in the phase and modulus of the pairing order parameter are absolutely necessary to give physically acceptable chemical potential and sound velocity. We presented analytical results for the change in concavity of the collective mode dispersion from convex to concave as contact interactions are changed from the BCS to the Bose regime. The dispersion never hits the two-particle continuum threshold, due to the existence of two-body bound states for arbitrarily small attractive s-wave interactions in two dimensions.

---

*Senne.Van_Loon@colostate.edu

[1] J. Goldstone, Field theories with superconductor solutions, Nuovo Cimento **19**, 154 (1961).

[2] P. W. Higgs, Spontaneous symmetry breakdown without massless bosons, Phys. Rev. **145**, 1156 (1966).

[3] F. Englert, R. Brout, and M. F. Thiry, Vector mesons in presence of broken symmetry, Nuovo Cimento A **43**, 244 (1966).

[4] T. Hong, M. Matsumoto, Y. Qiu, W. Chen, T. R. Gentile, S. Watson, F. F. Awwadi, M. M. Turnbull, S. E. Dissanayake, H. Agrawal, R. Toft-Petersen, B. Klemke, K. Coester, K. P. Schmidt, and D. A. Tennant, Higgs amplitude mode in a two-dimensional quantum antiferromagnet near the quantum critical point, Nat. Phys. **13**, 638 (2017).

[5] S. Maiti and P. J. Hirschfeld, Collective modes in superconductors with competing s- and d-wave interactions, Phys. Rev. B **92**, 094506 (2015).

[6] V. Greco, M. Colonna, M. Di Toro, and F. Matera, Collective modes of asymmetric nuclear matter in quantum hadrodynamics, Phys. Rev. C **67**, 015203 (2003).

[7] N. Yamamoto, M. Tachibana, T. Hatsuda, and G. Baym, Phase structure, collective modes, and the axial anomaly in dense QCD, Phys. Rev. D **76**, 074001 (2007).

[8] D. Kobyakov and C. J. Pethick, Dynamics of the inner crust of neutron stars: Hydrodynamics, elasticity, and collective modes, Phys. Rev. C **87**, 055803 (2013).

[9] S. D. Mathur and D. Turton, Comments on black holes I: The possibility of complementarity, J. High Energy Phys. 01 (2014) 034.

[10] V. P. Singh and L. Mathey, Collective modes and superfluidity of a two-dimensional ultracold Bose gas, Phys. Rev. Res. **3**, 023112 (2021).

[11] S. Choudhury, K. R. Islam, Y. Hou, J. A. Aman, T. C. Killian, and K. R. A. Hazzard, Collective modes of ultracold fermionic alkaline-earth-metal gases with SU(N) symmetry, Phys. Rev. A **101**, 053612 (2020).

[12] C. Chin, R. Grimm, P. Julienne, and E. Tiesinga, Feshbach resonances in ultracold gases, Rev. Mod. Phys. **82**, 1225 (2010).

[13] E. Ibarra-García-Padilla, R. Mukherjee, R. G. Hulet, K. R. A. Hazzard, T. Paiva, and R. T. Scalettar, Thermodynamics and magnetism in the two-dimensional to three-dimensional crossover of the Hubbard model, Phys. Rev. A **102**, 033340 (2020).

[14] N. D. Mermin and H. Wagner, Absence of Ferromagnetism or Antiferromagnetism in One- or Two-Dimensional Isotropic Heisenberg Models, Phys. Rev. Lett. **17**, 1133 (1966).

[15] P. C. Hohenberg, Existence of long-range order in one and two dimensions, Phys. Rev. **158**, 383 (1967).

[16] V. L. Berezinskii, Destruction of long-range order in one-dimensional and two-dimensional systems possessing a continuous symmetry group. II. Quantum systems, Sov. Phys. JETP **34**, 610 (1972).

[17] J. M. Kosterlitz and D. J. Thouless, Long range order and metastability in two dimensional solids and superfluids. (Application of dislocation theory), J. Phys. C **5**, L124 (1972).

[18] B. Keimer, S. A. Kivelson, M. R. Norman, S. Uchida, and J. Zaanen, From quantum matter to high-temperature superconductivity in copper oxides, Nature (London) **518**, 179 (2015).

[19] J.-F. Ge, Z.-L. Liu, C. Liu, C.-L. Gao, D. Qian, Q.-K. Xue, Y. Liu, and J.-F. Jia, Superconductivity above 100 K in single-layer FeSe films on doped $SrTiO_3$, Nat. Mater. **14**, 285 (2015).

[20] Y. Cao, V. Fatemi, S. Fang, K. Watanabe, T. Taniguchi, E. Kaxiras, and P. Jarillo-Herrero, Unconventional superconductivity in magic-angle graphene superlattices, Nature (London) **556**, 43 (2018).

[21] Y. Yu, L. Ma, P. Cai, R. Zhong, C. Ye, J. Shen, G. D. Gu, X. H. Chen, and Y. Zhang, High-temperature superconductivity in monolayer $Bi_2Sr_2CaCu_2O_{8+\delta}$, Nature (London) **575**, 156 (2019).

[22] V. Makhalov, K. Martiyanov, and A. Turlapov, Ground-State Pressure of Quasi-2D Fermi and Bose Gases, Phys. Rev. Lett. **112**, 045301 (2014).

[23] K. Fenech, P. Dyke, T. Peppler, M. G. Lingham, S. Hoinka, H. Hu, and C. J. Vale, Thermodynamics of an Attractive 2D Fermi Gas, Phys. Rev. Lett. **116**, 045302 (2016).

[24] I. Boettcher, L. Bayha, D. Kedar, P. A. Murthy, M. Neidig, M. G. Ries, A. N. Wenz, G. Zürn, S. Jochim, and T. Enss, Equation of State of Ultracold Fermions in the 2D BEC-BCS Crossover Region, Phys. Rev. Lett. **116**, 045303 (2016).

[25] Z. Hadzibabic, P. Krüger, M. Cheneau, B. Battelier, and J. Dalibard, Berezinskii-Kosterlitz-Thouless crossover in a trapped atomic gas, Nature (London) **441**, 1118 (2006).

[26] P. A. Murthy, I. Boettcher, L. Bayha, M. Holzmann, D. Kedar, M. Neidig, M. G. Ries, A. N. Wenz, G. Zürn, and S. Jochim, Observation of the Berezinskii-Kosterlitz-Thouless Phase Transition in an Ultracold Fermi Gas, Phys. Rev. Lett. **115**, 010401 (2015).

[27] J. L. Ville, R. Saint-Jalm, É. Le Cerf, M. Aidelsburger, S. Nascimbène, J. Dalibard, and J. Beugnon, Sound Propagation in a Uniform Superfluid Two-Dimensional Bose Gas, Phys. Rev. Lett. **121**, 145301 (2018).

[28] M. Bohlen, L. Sobirey, N. Luick, H. Biss, T. Enss, T. Lompe, and H. Moritz, Sound Propagation and Quantum-Limited Damping in a Two-Dimensional Fermi Gas, Phys. Rev. Lett. **124**, 240403 (2020).

[29] P. Christodoulou, M. Gałka, N. Dogra, R. Lopes, J. Schmitt, and Z. Hadzibabic, Observation of first and second sound in a BKT superfluid, Nature (London) **594**, 191 (2021).

[30] L. Sobirey, H. Biss, N. Luick, M. Bohlen, H. Moritz, and T. Lompe, Observing the Influence of Reduced Dimensionality on Fermionic Superfluids, Phys. Rev. Lett. **129**, 083601 (2022).

[31] K. Martiyanov, V. Makhalov, and A. Turlapov, Observation of a Two-Dimensional Fermi Gas of Atoms, Phys. Rev. Lett. **105**, 030404 (2010).

[32] M. Feld, B. Fröhlich, E. Vogt, M. Koschorreck, and M. Köhl, Observation of a pairing pseudogap in a two-dimensional Fermi gas, Nature (London) **480**, 75 (2011).

[33] P. Dyke, E. D. Kuhnle, S. Whitlock, H. Hu, M. Mark, S. Hoinka, M. Lingham, P. Hannaford, and C. J. Vale, Crossover from 2D to 3D in a Weakly Interacting Fermi Gas, Phys. Rev. Lett. **106**, 105304 (2011).

[34] W. Ong, C. Cheng, I. Arakelyan, and J. E. Thomas, Spin-Imbalanced Quasi-Two-Dimensional Fermi Gases, Phys. Rev. Lett. **114**, 110403 (2015).

[35] K. Hueck, N. Luick, L. Sobirey, J. Siegl, T. Lompe, and H. Moritz, Two-Dimensional Homogeneous Fermi Gases, Phys. Rev. Lett. **120**, 060402 (2018).

[36] S. Hoinka, P. Dyke, M. G. Lingham, J. J. Kinnunen, G. M. Bruun, and C. J. Vale, Goldstone mode and pair-breaking excitations in atomic Fermi superfluids, Nat. Phys. **13**, 943 (2017).

[37] H. Biss, L. Sobirey, N. Luick, M. Bohlen, J. J. Kinnunen, G. M. Bruun, T. Lompe, and H. Moritz, Excitation Spectrum and Superfluid Gap of an Ultracold Fermi Gas, Phys. Rev. Lett. **128**, 100401 (2022).

[38] M. Randeria, J.-M. Duan, and L.-Y. Shieh, Superconductivity in a two-dimensional Fermi gas: Evolution from Cooper pairing to Bose condensation, Phys. Rev. B **41**, 327 (1990).

[39] M. Marini, F. Pistolesi, and G. Strinati, Evolution from BCS superconductivity to Bose condensation: Analytic results for the crossover in three dimensions, Eur. Phys. J. B **1**, 151 (1998).

[40] L. Salasnich, P. A. Marchetti, and F. Toigo, Superfluidity, sound velocity, and quasicondensation in the

two-dimensional BCS-BEC crossover, Phys. Rev. A **88,** 053612 (2013).

[41] L.-P. Lumbeeck, J. Tempere, and S. Klimin, Dispersion and damping of phononic excitations in Fermi superfluid gases in 2D, Condens. Matter **5,** 13 (2020).

[42] L. He, H. Lü, G. Cao, H. Hu, and X.-J. Liu, Quantum fluctuations in the BCS-BEC crossover of two-dimensional Fermi gases, Phys. Rev. A **92,** 023620 (2015).

[43] G. Bighin and L. Salasnich, Finite-temperature quantum fluctuations in two-dimensional Fermi superfluids, Phys. Rev. B **93,** 014519 (2016).

[44] V. N. Popov, *Functional Integrals and Collective Excitations* (Cambridge University Press, Cambridge, England, 1991).

[45] R. Combescot, M. Y. Kagan, and S. Stringari, Collective mode of homogeneous superfluid Fermi gases in the BEC-BCS crossover, Phys. Rev. A **74,** 042717 (2006).

[46] H. Kurkjian, Y. Castin, and A. Sinatra, Concavity of the collective excitation branch of a Fermi gas in the BEC-BCS crossover, Phys. Rev. A **93,** 013623 (2016).

[47] J. R. Engelbrecht, M. Randeria, and C. A. R. Sá de Melo, BCS to Bose crossover: Broken-symmetry state, Phys. Rev. B **55,** 15153 (1997).

[48] S. S. Botelho and C. A. R. Sá de Melo, Vortex-Antivortex Lattice in Ultracold Fermionic Gases, Phys. Rev. Lett. **96,** 040404 (2006).

[49] D. S. Petrov and G. V. Shlyapnikov, Interatomic collisions in a tightly confined Bose gas, Phys. Rev. A **64,** 012706 (2001).

[50] P. Nozières and S. Schmitt-Rink, Bose condensation in an attractive fermion gas: From weak to strong coupling superconductivity, J. Low Temp. Phys. **59,** 195 (1985).

[51] C. A. R. Sá de Melo, M. Randeria, and J. R. Engelbrecht, Crossover from BCS to Bose Superconductivity: Transition Temperature and Time-Dependent Ginzburg-Landau Theory, Phys. Rev. Lett. **71,** 3202 (1993).

[52] Note that one has to introduce convergence factors to regularize the Matsubara sum in the thermodynamic potential Ω_g. This is most easily done in the basis of the real and imaginary part of the pair field Φ, instead of the phase-modulus basis used here [42,47].

[53] See Supplemental Material at http://link.aps.org/supplemental/10.1103/PhysRevLett.131.113001 for a more detailed description on damping of collective modes, the poles of the structure factor, and the differences between the sound velocity of the broken U(1) symmetry and Landau's first and second sound. The Supplemental Material includes Refs. [54–65].

[54] S. T. Beliaev, Energy spectrum of non-ideal Bose gas, Sov. Phys. JETP **34,** 299 (1958).

[55] L. Landau and I. Khalatnikov, The theory of the viscosity of helium II. I. Collisions of elementary excitations in helium II, Zh. Eksp. Teor. Fiz. **19,** 637 (1949).

[56] M. A. H. Tucker and A. F. G. Wyatt, Four-phonon scattering in superfluid ^{4}He, J. Phys. Condens. Matter **4,** 7745 (1992).

[57] I. N. Adamenko, Y. A. Kitsenko, K. E. Nemchenko, and A. F. G. Wyatt, Theory of scattering between two phonon beams in superfluid helium, Phys. Rev. B **80,** 014509 (2009).

[58] D. M. Stamper-Kurn, H.-J. Miesner, S. Inouye, M. R. Andrews, and W. Ketterle, Collisionless and Hydrodynamic Excitations of a Bose-Einstein Condensate, Phys. Rev. Lett. **81,** 500 (1998).

[59] C. Buggle, P. Pedri, W. von Klitzing, and J. T. M. Walraven, Shape oscillations in nondegenerate Bose gases: Transition from the collisionless to the hydrodynamic regime, Phys. Rev. A **72,** 043610 (2005).

[60] H. Kurkjian, Y. Castin, and A. Sinatra, Landau-Khalatnikov phonon damping in strongly interacting Fermi gases, Europhys. Lett. **116,** 40002 (2016).

[61] Y. Castin, Bragg spectroscopy and pair-breaking-continuum mode in a superfluid Fermi gas, arXiv:1911.10950v3.

[62] H. Kurkjian, J. Tempere, and S. N. Klimin, Linear response of a superfluid Fermi gas inside its pair-breaking continuum, Sci. Rep. **10,** 11591 (2020).

[63] H. Hu, E. Taylor, X.-J. Liu, S. Stringari, and A. Griffin, Second sound and the density response function in uniform superfluid atomic gases, New J. Phys. **12,** 043040 (2010).

[64] R. P. Feynman, Atomic theory of the two-fluid model of liquid helium, Phys. Rev. **94,** 262 (1954).

[65] L. Landau, Theory of the superfluidity of Helium II, Phys. Rev. **60,** 356 (1941).

[66] L. D. Landau and E. M. Lifshitz, *Quantum Mechanics*, 3rd ed. (Pergamon Press, New York, 1977), p. 63.

[67] H. Shi, S. Chiesa, and S. Zhang, Ground-state properties of strongly interacting Fermi gases in two dimensions, Phys. Rev. A **92,** 033603 (2015).

[68] L. Landau, Theory of the superfluidity of Helium II, J. Phys. USSR **5,** 71 (1941).

[69] P. C. Hohenberg and P. C. Martin, Superfluid Dynamics in the Hydrodynamic ($\omega\tau \ll 1$) and Collisionless ($\omega\tau \gg 1$) Domains, Phys. Rev. Lett. **12,** 69 (1964).

[70] P. C. Hohenberg and P. C. Martin, Microscopic theory of superfluid helium, Ann. Phys. (N.Y.) **34,** 291 (1965).